IOPscience iopscience.iop.org

Home Search Collections Journals About Contact us My IOPscience

Low-temperature magnetic and transport anisotropy in manganite thin films

This article has been downloaded from IOPscience. Please scroll down to see the full text article.

2009 J. Phys.: Condens. Matter 21 456002

(http://iopscience.iop.org/0953-8984/21/45/456002)

View the table of contents for this issue, or go to the journal homepage for more

Download details:
IP Address: 129.252.86.83
The article was downloaded on 30/05/2010 at 06:01

Please note that terms and conditions apply.

J. Phys.: Condens. Matter **21** (2009) 456002 (7pp) doi:10.1088/0953-8984/21/45/456002

Low-temperature magnetic and transport anisotropy in manganite thin films

A Iorio, C A Perroni, G De Filippis, V Marigliano Ramaglia and V Cataudella

CNR-INFM Coherentia and Università degli Studi di Napoli Federico II, Dipartimento di Scienze Fisiche, Complesso Universitario Monte S Angelo, Via Cintia, I-80126 Napoli, Italy

E-mail: vittorio.cataudella@na.infn.it

Received 30 June 2009, in final form 16 September 2009
Published 21 October 2009
Online at stacks.iop.org/JPhysCM/21/456002

Abstract

The stability of striped magnetic phases in films of $La_{1-x}A_xMnO_3$ perovskites is investigated. A variational analysis is developed for different film thicknesses at fixed hole density ($x = 0.3$) and the competition among magnetic phases as a function of the transfer integral and the temperature is analyzed. The stabilization of an in-plane striped magnetic phase is observed with reducing the film thickness at low temperatures below the metal–insulator transition temperature. Within the adopted variational scheme, treating perturbatively the residual electron–phonon interaction, the dependence of the in-plane resistivity on temperature for different thicknesses is calculated. At low temperatures, due to the striped magnetic phase, the resistivity shows an important in-plane anisotropy. The obtained results are found to be consistent with experiments.

(Some figures in this article are in colour only in the electronic version)

1. Introduction

The perovskite oxides $La_{1-x}A_xMnO_3$ (A stands for a divalent alkali element such as Sr or Ca) have been studied intensively since the discovery of 'colossal' magneto-resistance (CMR) in thin films [1]. Dramatic changes in electron and magnetic properties are found at temperatures around the combined ferromagnetic–paramagnetic and metal–insulator (MI) transitions. The ferromagnetic phase is usually explained by introducing the double-exchange mechanism [2], in which hopping of an outer shell electron from a Mn^{3+} to a Mn^{4+} site is favored by a parallel alignment of the core spins. In addition to the double-exchange term that promotes hopping of the carriers, a significant interaction between electrons and lattice distortions plays a non-negligible role in these compounds [3–7]. Actually, for the Mn^{3+} site, with three electrons in the energetically lower spin triplet state t_{2g} and the mobile electron in the higher doublet e_g, a Jahn–Teller distortion of the oxygen octahedron can lead to splitting of the doublet and the trapping of the charge carriers in a polaronic state.

The physics of these compounds is very rich and even more complex in the case of films, where the role of vertical confinement, strain and disorder is crucial [8, 9]. In particular, the interface between the films and the substrate can play an important role, giving rise to phase separated regions with different magnetic structures and affecting the transport properties especially in very thin films. Recently, a number of experimental observations in thin films have been reported showing an unexpected strong anisotropy in the in-plane properties [10–12] below the MI transition[1]. For very thin films (thickness < 100 Å) of $La_{1-x}Sr_xMnO_3$ (LSMO), grown on different substrates, the resistance curves $R(T)$, along the *ab* crystallographic axes, have been found remarkably different. In particular along one of the crystallographic directions the $R(T)$ curve exhibits a 'bump' at temperatures around 120 K while along the other one the behavior of the resistivity appears very close to the one expected for thicker films and bulk samples: metallic up to 320 K. On the other hand, for thick (>400 Å) films, the resistance curves in different directions of the *ab*-plane did not show sizable differences. The observed anisotropy in the resistance has been attributed to the substrate interface that can exhibit step-like terraces [12, 10]. However,

[1] Above the MI transition temperature the LSMO films, regardless of their thickness and substrate, do not exhibit any anisotropy in the *ab*-plane. In the insulating phase the transport is dominated by the polaron formation triggered by the paramagnetic phase and by disorder that restores the *a*–*b* transport isotropy.

 © 2009 IOP Publishing Ltd Printed in the UK

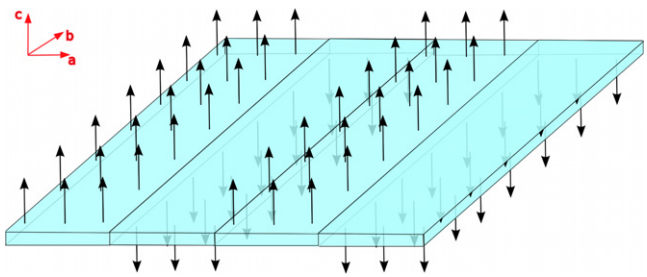

Figure 1. The picture schematically shows the magnetic-stripe order corresponding to in-plane anisotropic magnetic solutions.

the persistence of the effect with changing the substrate makes this suggestion doubtful.

In this paper, we show that an alternative explanation is possible based on the formation of *magnetic-stripe* phase (MS). We discuss the stability of such a phase without assuming any extrinsic effect at the interface with the substrate. As we will show, indeed, a MS phase can form. The magnetic physical origin of the observed anisotropy stems from several experimental observations that suggest the existence of a 'dead layer', at the interface with the substrate, exhibiting an insulating non-ferromagnetic behavior [13, 14]. A further insight into the problem comes from the well-known observation that these compounds exhibit a strong tendency towards ferromagnetic and antiferromagnetic nanoscopic phase separation [15, 16]. Finally, it is worth noticing that the possible existence of extrinsic effects can work as a further stabilizing factor for the magnetic phase we discuss.

In MS phases we assume that the order of the t_{2g} spin is such that ferromagnetic stripes alternate with the opposite magnetization (see figure 1). The transverse size of each stripe is a free parameter to be determined by energetic considerations. The numerical comparison with the isotropic phases (ferromagnetic (FM) and G-type antiferromagnetic (AFM) phases) allows us to build up a phase diagram in the plane defined by the transfer integral (hopping amplitude) between nearest-neighbor sites, t, and temperature, T. In our analysis the hopping amplitude plays an important role since its variations are able to model the presence of strain in the film [8]. Phase diagrams are obtained for different thicknesses (figures 2 and 3). We have observed that the stability region for the anisotropic phase moves slightly towards larger values of t with increasing film thickness and reaches a saturation limit around 100 planes. At the same time, for small values of T the magnetic-stripe phase becomes wider. We have also calculated the film resistivity as a function of the temperature at fixed values of hopping, for different sizes, recovering the in-plane anisotropy observed in the experiments. The anisotropy is obtained when the transition from ferromagnetic to magnetic-stripe phase takes place.

In section 2 the model is introduced and the adopted variational approach reviewed. In section 3 the behavior of the resistivity in the ab-plane as a function of temperature is reported and discussed. Finally, in section 4, the conclusions are reported.

2. The model and the variational approach

We adopt the so-called single orbital approximation for manganite. This model, qualitatively accurate for $x < 0.5$, describes the dynamics of the e_g electrons subjected to the double-exchange mechanism and coupled to the lattice distortions. It also takes into account super-exchange interaction between neighboring localized t_{2g} electrons. The coupling to longitudinal optical phonons arises from the Jahn–Teller effect that splits the e_g double degeneracy [17]. Then the Hamiltonian reads

$$H = -t\sum_{i,\vec{\delta}}\left(\frac{S_0^{i,i+\vec{\delta}}+1/2}{2S+1}\right)c_i^\dagger c_{i+\vec{\delta}} + \omega_0\sum_i a_i^\dagger a_i + g\omega_0\sum_i c_i^\dagger c_i(a_i+a_i^\dagger) + \frac{\epsilon}{2}\sum_{i,\vec{\delta}}\vec{S}_i\cdot\vec{S}_{i+\vec{\delta}} - \mu\sum_i c_i^\dagger c_i. \quad (1)$$

Here t is the transfer integral of electrons occupying e_g orbitals between nearest-neighbor (nn) sites, $S_0^{i,i+\vec{\delta}}$ is the total spin of the subsystem consisting of two localized spins on nn sites and the conduction electron, $\vec{S}_i$ is the spin of the t_{2g} core states ($S = 3/2$) and $c_i^\dagger(c_i)$ creates (destroys) an electron with spin parallel to the ionic spin at the ith site in the e_g orbital. The coordination vector $\vec{\delta}$ connects nn sites. The first term of the Hamiltonian describes the double-exchange mechanism in the limit where the intra-atomic exchange integral J is far larger than the transfer integral t. Furthermore in equation (1) ω_0 denotes the frequency of the local optical phonon mode, $a_i^\dagger(a_i)$ is the creation (annihilation) phonon operator at the site i, the dimensionless parameter g indicates the strength of the electron–phonon interaction in the Holstein model [18], ϵ represents the antiferromagnetic super-exchange coupling between two nn t_{2g} spins and μ is the chemical potential. The hopping of electrons is supposed to take place between the equivalent nn sites of a simple cubic lattice separated by the distance $|n - n'| = a$. The units are such that the Planck constant $\hbar = 1$, the Boltzmann constant $k_B = 1$ and the lattice parameter $a = 1$. In order to treat the electron–phonon interaction variationally, we use a scheme already proposed in a similar context [19] based on a modified Lang–Firsov canonical transformation and the Bogoliubov inequality [20, 21]. The latter allows us to fix an upper limit for the free energy F:

$$F \leqslant F_{\text{test}} + \langle\tilde{H} - H_{\text{test}}\rangle_t, \quad (2)$$

where F_{test} and H_{test} are the free energy and the Hamiltonian corresponding to the model that has been assumed as the ansatz. The symbol $\langle\,\rangle_t$ indicates a thermodynamic average performed by using the test Hamiltonian.

Following [17], we choose H_{test} in such a way that electron, phonon and spin degrees of freedom are not interacting:

$$H_{\text{test}} = H_{\text{test}}^{\text{el}} + \omega_0\sum_i a_i^\dagger a_i + N\omega_0 g^2(1-x)^2(1-f)^2 - g_s\mu_B\sum_i\vec{h}_{\text{eff}}\cdot\vec{S}_i. \quad (3)$$

Here $N = N_x N_y N_z$ is total number of the lattice sites, g_s is the dimensionless electron spin factor ($g_s \simeq 2$) and μ_B is the Bohr magneton. Furthermore, f and $h_{\rm eff}$ represent, respectively, the polaron localization parameter and the effective molecular magnetic field that are determined by the variational approach. In the test Hamiltonian (3), $H^{\rm el}_{\rm test}$ reads

$$H^{\rm el}_{\rm test} = -t\mathrm{e}^{-S_T} \sum_{i,\vec{\delta}} \gamma_{\vec{\delta}} c_i^\dagger c_{i+\vec{\delta}} - \mu_{\rm eff} \sum_i c_i^\dagger c_i, \qquad (4)$$

where the factor e^{-S_T} controls the band renormalization due to the polaron formation and $\gamma_{\vec{\delta}}$ indicates the thermal average of the double-exchange spin operator

$$\gamma_{\vec{\delta}} = \left\langle \left(\frac{S_0^{i,i+\vec{\delta}} + 1/2}{2S+1} \right) \right\rangle_t, \qquad (5)$$

that depends on the relative orientation of the t_{2g} spin localized on (nn) sites. Furthermore, $\mu_{\rm eff}$ represents the effective chemical potential. From the inequality (2) we obtain the variational free energy for a single site:

$$\frac{F}{N} = f^{\rm el}_{\rm test} + T\log(1-\mathrm{e}^{-\beta\omega_0}) + \omega_0 g^2 (1-f)^2 (1-x)^2 - T\log v_S + f^{\rm ord}_{\rm test} + T\lambda m_S, \qquad (6)$$

where $f^{\rm el}_{\rm test}$ represents the electronic contribution to the free energy and $f^{\rm ord}_{\rm test}$ depends on the magnetic order of the system. Both will be discussed in some detail in the following. In equation (6) β is the inverse of the temperature, v_S is the partition function of the localized spins, λ is a dimensionless variational parameter proportional to the effective magnetic field.

In order to calculate $f^{\rm el}_{\rm test}$, we need to know the energy spectrum of $H_{\rm test}$. In particular we have to calculate the associated electronic eigenvalues. This calculation is carried out by diagonalizing the electronic contribution to the test Hamiltonian. For MS solutions the derivation of the electron dispersion relation has to take into account the periodic nature of the solution. Actually, this solution introduces a positional dependence of the double-exchange factor that, in turn, modulates the effective transfer integral. In order to fix the ideas, we assume the x-axis as the direction along which the MS alternate (a-direction). Assuming that the transverse width of a single stripe is L, the corresponding dimension of the magnetic unit cell will be $(2L, 1, 1)$. As mentioned above, we need to diagonalize the electronic part of $H_{\rm test}$

$$H^{\rm el}_{\rm test}|k_x k_y k_z, \alpha\rangle = \xi(k_x, k_y, k_z, \alpha)|k_x k_y k_z, \alpha\rangle. \qquad (7)$$

Here k_x, k_y, k_z indicate the wavevectors of the magnetic lattice, α is the index of the magnetic unit cell and $\xi(k_x, k_y, k_z, \alpha)$ the electronic dispersion. In the ab-plane, we employ periodic boundary conditions. On the other hand, the finite size of the film is taken into account considering the system made of a finite number of planes and imposing open boundary conditions along the out-of-plane direction of growth [8]. The eigenvalue equation (7) with the boundary conditions mentioned above is equivalent to diagonalizing the following matrix $2L \times 2L$

$$\begin{pmatrix} D(k_y,k_z) & F & \cdots & E\mathrm{e}^{-\mathrm{i}2Lk_x} \\ F & D(k_y,k_z) & \cdots & 0 \\ \vdots & \vdots & \ddots & \vdots \\ E\mathrm{e}^{\mathrm{i}2Lk_x} & 0 & \cdots & D(k_y,k_z) \end{pmatrix},$$

where

$$F = -t\mathrm{e}^{-S_T}\gamma_{\delta_y} \qquad E = -t\mathrm{e}^{-S_T}\gamma_{\delta_x} \qquad (8)$$

represent the effective transfer integrals (5) for nearest-neighboring t_{2g} spin aligned and anti-aligned, respectively, while

$$D(k_y, k_z) = 2F(\cos(k_y) + \cos(k_z)) \qquad (9)$$

represents the partial dispersion relation connected to directions where the t_{2g} spin are aligned. The electron free energy for a generic solution reads

$$f^{\rm el}_{\rm test} = -\frac{T}{(2\pi)^2 N_z} \times \sum_{k_z}\sum_{\alpha} \int_{-\frac{\pi}{2L}}^{\frac{\pi}{2L}} \mathrm{d}k_x \int_{-\pi}^{\pi} \mathrm{d}k_y \log(1+\mathrm{e}^{-\beta\xi(\mathbf{k},\alpha)}). \qquad (10)$$

In equation (10) N_z is the number of planes in the z direction.

We have analyzed the behavior of the MS solutions with different transverse widths L. In particular, $L = 1$ has been compared with $L = 2$ and 3 (this last case is sketched in figure 1). In every case, in the magnetic super-cell, we stress that there is only one antiferromagnetic bond along the x-axis. The solutions differ from each other for the number of the ferromagnetic bonds: 0 for $L = 1$, 2 for $L = 2$, 4 for $L = 3$. In the parameter range where the antiferromagnetic solutions are favored (smaller t), the solution with $L = 1$ becomes more stable in comparison with MS phases characterized by larger values of L. On the contrary, in the parameter range where ferromagnetic solutions are favored (larger t), phases with larger value of L have lower energies with respect to the case $L = 1$. However, in this case, the phases with L larger than 1 always have energies higher than those of the homogeneous ferromagnetic phase by varying the parameter hopping t, temperature T and number of planes N_z in the z direction. Therefore, the most stable solution, among the MS ones, corresponds to that with the minimal transverse width of the stripes ($L = 1$).[2] For this magnetic order we can exhibit the electronic band in a closed form:

$$\xi_{\mathbf{k}} = E\cos(k_x) + F\cos(k_y) + F\cos(k_z) - \mu_{\rm eff}. \qquad (11)$$

For $L = 1$ we obtain also a simple compact form for $f^{\rm ord}_{\rm test}$:

$$f^{\rm ord}_{\rm test} = \left(\pm 3 - \frac{1}{N_z}\right) \varepsilon S^2 m_S^2, \qquad (12)$$

[2] In the case $L = 1$ the MS phase reduces to the so-called A-type AFM phase. This is the magnetic configuration closest to the homogeneous FM phase that is stabilized for thicker films. Different magnetic configurations like C-type AFM have higher energies at $x = 0.3$ [22].

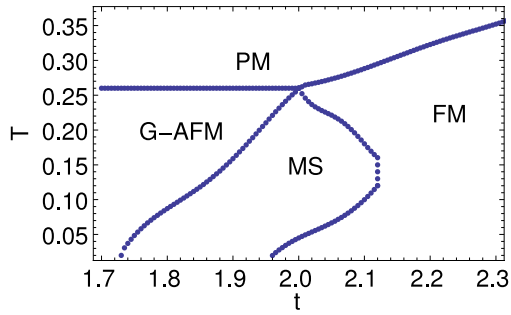

Figure 2. Phase diagram in the hopping–temperature plane for $N_z = 2$ at fixed hole density ($x = 0.3$), corresponding to $g = 2$ and $\varepsilon = 0.05\omega_0$. PM means paramagnetic metal, FM ferromagnetic metal, G-AFM G-type antiferromagnetic metal and finally MS indicates the magnetic-stripe solution. The transfer integral t and the temperature T are expressed in units of ω_0.

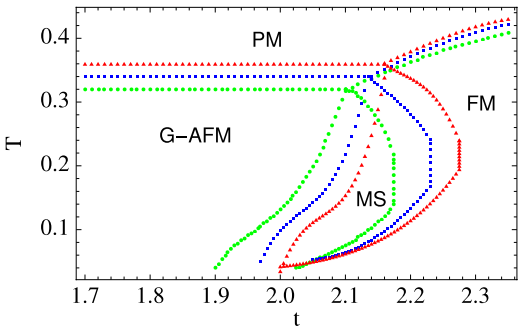

Figure 3. Comparison among the phase diagrams corresponding to different thicknesses: $N_z = 5$ (full circles, green), $N_z = 10$ (full squares, blue) and $N_z = 100$ (full triangles, red). PM means paramagnetic metal, FM ferromagnetic metal, G-AFM G-type antiferromagnetic metal and finally MS indicates the magnetic-stripe solution. The transfer integral t and the temperature T are expressed in units of ω_0.

where the top and bottom signs hold, respectively, for the ferromagnetic and antiferromagnetic solutions. While for the magnetic-stripe solution this becomes

$$f_{\text{test}}^{\text{ord}} = \left(1 - \frac{1}{N_z}\right) \varepsilon S^2 m_S^2. \tag{13}$$

In our study an important role is played by the hopping amplitude. Actually, the change of the hopping amplitude is able to trigger the stabilization of the MS phase. It is well known that there is a close connection between t and the biaxial strain due to the substrate. It has been carefully shown [10, 11] that in an epitaxial thin film of $La_{1-x}Ca_xMnO_3$, grown on substrates with significant tensile lattice mismatch, the in-plane parameter increases while the out-of-plane lattice constant is reduced. Similar results are also reported in [12], where the out-of-plane lattice parameter, c, in an LSMO epitaxial thin film was measured as a function of the film thickness showing a reduction of c for thinner films. These results suggest that when the film's thickness is smaller than 400 Å some tensile strain is present in the ab-plane. Consequently, the in-plane parameter increases and the hopping amplitude decreases. Summarizing, our conjecture is that the reduction of the thickness *drives* a reduction of the transfer integral.

In figure 2 we show the hopping amplitude–temperature phase diagram for the case of $N_z = 2$. It is clear that the anisotropic phase with ($L = 1$) stabilizes in a wide region between antiferromagnetic and ferromagnetic phases. The existence of the MS phase can be understood as a reasonable compromise between the two homogeneous phases that at their interface exhibit a higher energy. Furthermore, the phase separation between magnetically ordered and paramagnetic phases is not modified by the presence of the MS phase, suggesting that the MI transition (driven by the ferromagnetic–paramagnetic (FM–PM) transition) is not modified by the stabilization of the MS phase. It is also notable that the *re-entrant* shape of the stability region for the MS phase determines, for suitable values of hopping amplitude t, an interesting sequence of order–order transition: FM $\mapsto$ MS and MS $\mapsto$ FM. Finally, we would emphasize that our numerical results, for the set of parameters used in this work and suitable for LSMO [12], provide itinerant wavefunctions for the electrons. The mass renormalization, due to the electron–phonon coupling, is not very large and we do not see any polaron self-trapping in the magnetically ordered phases.

Moreover we have studied the stability of the MS phase (see figure 3) for different numbers of planes and we have found that the MS phase moves slightly towards larger t values when the number of layers increases, saturating at around 100 layers. We also observe that, at very low temperatures, the range of hopping, where the MS solution stabilizes, decreases as the number of layers increases.

It is worth noticing that, starting from a value of the hopping amplitude corresponding to the region where FM stabilizes, the MS phase stabilizes, reducing the hopping amplitude. In our numerical results the extent of reduction of hopping amplitude that leads to transition FM $\mapsto$ MS is compatible to the typical extent of in-plane lattice parameter caused by tensile strain. We end this section with a general remark on the anisotropy observed in thin films of LSMO grown on different substrates. As a matter of fact, for suitable values of hopping, where the MS stabilizes, we have shown that an anisotropic behavior in the in-plane properties of the film occurs. How can this be linked to the experimental data? As already mentioned, for epitaxial thin film coherently strained by in-plane tensile strain and for thickness such that the mismatch causes an increase of the in-plane lattice parameter, we expect a decrease of the effective hopping amplitude. Actually, even for moderate compressive strain, a decrease of the c-axis has been observed in those very thin films exhibiting anisotropic behavior. This suggests to us that, also in this case, the effective hopping amplitude could decrease.

3. Resistivity: in-plane anisotropy

In order to show that the stabilization of the MS phase can, indeed, lead to the anisotropy observed experimentally we calculate, in this section, the resistivity for temperatures lower than the FM $\mapsto$ PM transition.

It is well known that the resistivity is given by the inverse of the $\omega \mapsto 0$ limit of the real part of $\sigma_{\alpha,\alpha}(\omega)$ that is related to the current–current correlation function, $\Pi^{\rm ret}_{\alpha,\alpha}(\omega)$, by

$$\mathrm{Re}\,\sigma_{\alpha,\alpha}(\omega) = -\frac{\mathrm{Im}\,\Pi^{\rm ret}_{\alpha,\alpha}(\omega)}{\omega}. \tag{14}$$

Therefore our problem reduces to evaluating the current–current correlation function. Following the scheme introduced in [17] and limiting our analysis only to the coherent contribution of the conductivity, it is possible to show that, in Matsubara frequencies, $\Pi^{\rm coh}_{\alpha,\alpha}(\mathrm{i}\omega_n)$ becomes

$$\Pi^{\rm coh}_{\alpha,\alpha}(\mathrm{i}\omega_n) = 4e^2t^2\mathrm{e}^{-2S_T}\left(\frac{1}{(2\pi)^2N_z}\right)\gamma^2_{\delta_\alpha}\sum_{k_z}\int_{-\pi}^{\pi}\mathrm{d}k_x \times \int_{-\pi}^{\pi}\mathrm{d}k_y\sin^2(k_\alpha)\int_0^\beta \mathrm{e}^{\mathrm{i}\omega_n\tau}\tilde{\mathcal{G}}(\mathbf{k},-\tau)\tilde{\mathcal{G}}(\mathbf{k},\tau), \tag{15}$$

where the index α refers to one of the two in-plane directions. We stress that in our approach Π depends on γ_{δ_α} defined in equation (5). The restriction to coherent processes for the current–current correlation function is justified at low temperatures where the multi-phonon in-coherent contribution is expected not to play a main role. We remember that, below the FM $\mapsto$ PM critical temperature, our variational analysis does not support the existence of phonon induced localization for the charge carriers that is, usually, associated with the incoherent transport. On the contrary, the charged electrons have an itinerant nature both in FM and MS phases. The situation changes in the high-temperature paramagnetic phase where the formation of small polarons is favored, giving rise to an insulating phase due to the cooperative effect of disorder.

Making the analytic continuation $\mathrm{i}\omega_n \to \omega + \mathrm{i}\delta$ in (15) and by using equation (14), it is possible to get the conductivity tensor and, hence, the in-plane resistivity, both along the stripes and perpendicular to them. However, in order to calculate the current–current correlation function (equation (15)) we still need a reasonable approximation for $\tilde{\mathcal{G}}$. Following [17] again, the Green's function can be carried out using the Lehmann representation

$$\tilde{\mathcal{G}}(\mathbf{k},\mathrm{i}\omega_n) = \int_{-\infty}^{+\infty}\frac{\mathrm{d}\omega}{2\pi}\frac{\tilde{A}(\mathbf{k},\omega)}{\mathrm{i}\omega_n-\omega} \tag{16}$$

and assuming for the spectral function $\tilde{A}$

$$\tilde{A}(\mathbf{k},\omega) = \frac{\Gamma(\mathbf{k})}{[\Gamma(\mathbf{k})]^2/4+(\omega-\xi_{\mathbf{k}})^2}, \tag{17}$$

with $\Gamma(\mathbf{k})$ corresponding to the itinerant polaron scattering rate. Due to the finite size along the z-axis, the contribution of the single phonon [19] to the scattering rate $\Gamma(\mathbf{k})$ reads

$$\Gamma_{1-\mathrm{phon}}(\mathbf{k}) = \sum_{k'_z}\left[t^2\mathrm{e}^{-2S_T}C^{\rm ord}(k_z,k'_z)I_1(s)\sinh\left(\frac{\beta\omega_0}{2}\right) + g^2\omega_0^2(1-f)^2\right]h(\mathbf{k},k'_z). \tag{18}$$

In equation (18) the dependence on magnetic solution is contained in the factor

$$C^{\rm ord}(k_z,k'_z) = 4(\gamma^2_{\delta_x}+\gamma^2_{\delta_y}+\gamma^2_{\delta_z})\Phi_1(k_z,k'_z) + (4\gamma^2_{\delta_x}+4\gamma^2_{\delta_y}+2\gamma^2_{\delta_z})\Phi_2(k_z,k'_z), \tag{19}$$

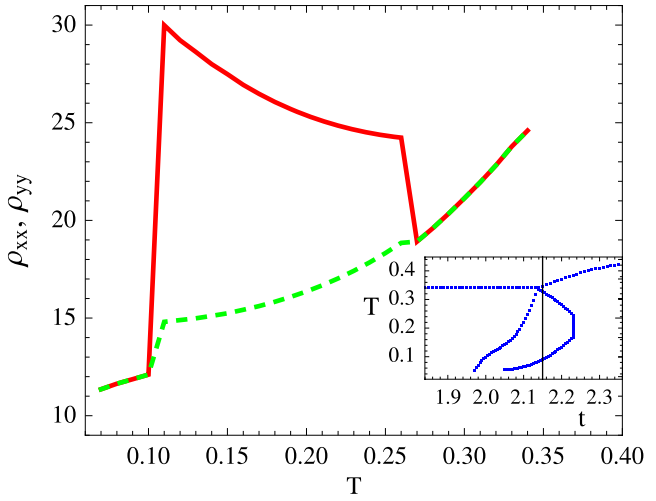

Figure 4. Resistivity versus temperature in the *ab*-plane for a five-layer thick film: ρ_{xx} (full line, red) and ρ_{yy} (dashed line, green) corresponding to $g = 2$ and $\varepsilon = 0.05\omega_0$ for a fixed value of hopping amplitude $t = 2.15\omega_0$. The resistivity is expressed in units of $\frac{e^2}{ah}$ and T in units of ω_0. In the inset the phase diagram (T–t), corresponding to five layers, is shown.

where $\Phi_1(k_z,k'_z)$ and $\Phi_2(k_z,k'_z)$ are given by

$$\Phi_1(k_z,k'_z) = \sum_{l=2}^{N_z-1}\phi^2(lk_z)\phi^2(lk'_z)$$
$$\Phi_2(k_z,k'_z) = \phi^2(k_z)\phi^2(k'_z)+\phi^2(N_zk_z)\phi^2(N_zk'_z) \tag{20}$$

and $\phi(lk_z)$ represents the projection of the electron eigenstates of the test Hamiltonian along the z-axis [8]. Moreover $h(\mathbf{k},k'_z)$ is given by

$$h(\mathbf{k},k'_z) = 2\pi\mathrm{e}^{-S_T}g(k'_z)[1+2n_{\rm B}(\omega_0) + n_{\rm F}(\omega_0+\xi_{\mathbf{k}})-n_{\rm F}(\xi_{\mathbf{k}}-\omega_0)], \tag{21}$$

where $n_{\rm B}$ and $n_{\rm F}$ indicate boson and fermion average occupation numbers, respectively. Furthermore $g(k'_z)$ is the constant density of states for fixed k'_z, while $I_1(s)$ is the modified Bessel function calculated for $s = 2f^2g^2[n_{\rm B}(\omega_0)(n_{\rm B}(\omega_0)+1)]^{1/2}$. It is worth noting that the single phonon scattering approximation has been already successfully used in the case of manganite films and bulk [8]. The reason why we can do this is that we have treated the residual electron–phonon interaction at the lowest order, after considering the interaction itself at the variational Lang–Firsov level.

In figures 4 and 5 we show the resistivity obtained by our approach. Clearly the resistivity exhibits a strong anisotropy depending whether the current is flowing along the stripes or perpendicular to them. The resistivity anisotropy is closely related to the magnetic transition FM $\mapsto$ MS.

Along the stripes the core spins are all aligned, both in the FM and MS phases, and the resistivity shows a metallic behavior very similar to the one expected in the homogeneous FM phase and observed in thicker films and bulk samples. On the other hand, along the direction perpendicular to the MS, where the spins are aligned in the FM phase and anti-aligned

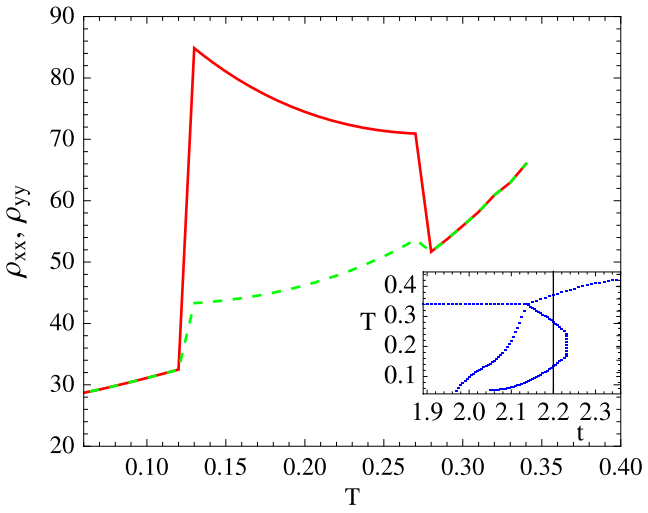

Figure 5. Resistivity versus temperature in the *ab*-plane for a ten-layer thick film: ρ_{xx} (full line, red) and ρ_{yy} (dashed line, green) corresponding to $g = 2$ and $\varepsilon = 0.05\omega_0$ for a fixed value of hopping amplitude $t = 2.2\omega_0$. The resistivity is expressed in units of $\frac{e^2}{a\hbar}$ and T in units of ω_0. In the inset the phase diagram (T–t), corresponding to ten layers, is shown.

in the MS phase, the resistivity jumps at the temperatures corresponding to the FM $\mapsto$ MS and MS $\mapsto$ FM transitions, respectively. The jumps are related to the different role played by the double exchange in the FM and MS phases. In the latter the antiferromagnetic order reduces the double-exchange effective transfer integral, thus reducing the mobility of the e_g electrons as is evident from equation (8). It should be noticed here that the abrupt jump could be related to the fact that disorder effects are not included in our analysis. Actually, disorder effects are able to smooth first-order transitions. In our case, therefore, disorder should be able to affect the transition between the ferromagnetic and MS phase. In any case, it is important to observe that the size of the jump (around a factor 2) is in good agreement with the value reported in the experiments. The reduction of the mobility of the e_g electrons in the MS phase is also confirmed by the insulating behavior exhibited by the resistivity along the direction perpendicular to the stripes. This behavior can be explained by the dependence on temperature of the double-exchange spin factor (5) for anti-aligned (nn) t_{2g} spin. Indeed, the latter increases as the temperature increases improving the mobility of the e_g electrons. For this reason the resistivity along such a direction decreases into the range where the MS solution stabilizes. Finally, in the range of temperatures where the ferromagnetic solution stabilizes again, the in-plane components of the resistivity tensor, along the MS and perpendicular to them, coincide and start to increase with temperature again.

4. Conclusions

We have analyzed the stability of the magnetic-stripe phases in thin films of $La_{1-x}A_xMnO_3$ perovskites. A variational approach previously proposed for manganite bulk and films has been generalized in order to consider magnetically anisotropic phases. It is found that a reduction of the e_g electron hopping between nn sites, t, stabilizes a phase characterized by ferromagnetic planes perpendicular to the substrate with alternating up and down magnetizations. This phase exhibits an interesting *re-entrant* behavior shape into the hopping–temperature plane determining, for suitable values of hopping, an interesting sequence of order–order transitions: FM $\mapsto$ MS and MS $\mapsto$ FM. Furthermore, we find that the stability region moves towards larger values of the hopping amplitude as the number of the planes increases, reaching saturation at around 100 planes. All these results can have an interesting impact on a number of experimental results showing a strong anisotropy in the low-temperature resistivity of very thin films. In fact, the strain induced by the substrate triggers a decrease of the lattice parameter that, in turns, suggests a reduction of the in-plane hopping. This is clearly understood for tensile strain but experimental data seem to indicate that it is true also for moderate compressive strain. As a matter of fact, the calculated resistivity tensor in the *ab*-plane shows an important anisotropy and reproduces the broad bump observed in the experiments at around 100 K. This structure is due to re-entrant behavior of the MS phase and, therefore, is triggered by the double-exchange mechanism. Indeed, in the range of temperatures where MS stabilizes, along the direction which presents anti-aligned t_{2g} spin, the resistivity decreases as temperature increases because the double-exchange effective hopping is reduced. On the other hand, along the direction parallel to the stripes, the resistivity exhibits the expected metallic behavior.

It is worth noticing that all the results presented in this work have been obtained without assuming any extrinsic effect at the interface with the substrate. It is reasonable to believe that the possible existence of extrinsic effects can work as a further stabilizing factor for the MS phase. In the case of very thin films, the interplay between intrinsic and extrinsic effects can become stronger, possibly giving rise to more complex magnetic patterns. The inclusion of the extrinsic effects in the analysis would require the proper study of the interface between film and substrate, which, in the present work, is taken into account in an average way by assuming a reduction of the in-plane effective electron hopping.

Finally, it is important to note that in our analysis the role of the double-exchange mechanism is studied at the level of variational mean-field, which includes the main contribution needed to stabilize the MS phases. More accurate approaches should take into account the role of the scattering of electrons by magnons [23]. This could affect the temperature profile of the resistivity, but not the anisotropy in different directions. Work to include magnon scattering in the calculation of the resistivity of the MS phase is in progress.

Acknowledgments

Valuable discussions with L Maritato and P Orgiani are gratefully acknowledged.

References

[1] von Helmolt A, Wecker J, Holzapfel B, Schultz L and Samwer K 1993 *Phys. Rev. Lett.* **71** 2331
Jin S, Tiefel T H, McCormack M, Fastnacht R A, Ramesh R and Chen L H 1994 *Science* **264** 413

[2] Zener C 1951 *Phys. Rev.* **81** 440
Zener C 1951 *Phys. Rev.* **82** 403
Anderson P W and Hasegawa H 1955 *Phys. Rev.* **100** 675
de Gennes P G 1960 *Phys. Rev.* **118** 141

[3] Millis A J, Littlewood P B and Shraiman B I 1995 *Phys. Rev. Lett.* **74** 5144
Millis A J, Shraiman B I and Mueller R 1996 *Phys. Rev. Lett.* **77** 175

[4] Millis A J 1998 *Nature* **392** 147

[5] Zhao G-M, Coder K, Keller H and Muller K A 1996 *Nature* **381** 676

[6] Lanzara A, Saini N L, Brunelli M, Natali F, Bianconi A, Radaelli P G and Cheong S W 1998 *Phys. Rev. Lett.* **81** 878

[7] Kim K H, Gu J Y, Choi H S, Park G W and Noh T W 1996 *Phys. Rev. Lett.* **77** 1877

[8] Perroni C A, Cataudella V, De Filippis G, Iadonisi G, Marigliano Ramaglia V and Ventriglia F 2003 *Phys. Rev.* B **68** 224424

[9] Mercone S *et al* 2005 *Phys. Rev.* B **71** 064415

[10] Klein J, Philipp J B, Reisinger D, Opel M, Marx A, Erb A, Alff L and Gross R 2003 *J. Appl. Phys.* **93** 7373

[11] Klein J, Philipp J B, Carbone G, Vigliante A, Alff L and Gross R 2002 *Phys. Rev.* B **66** 052414

[12] Orgiani P *et al* 2006 *Phys. Rev.* B **74** 134419

[13] Huijben M, Martin L W, Chu Y-H, Holcomb M B, Yu P, Rijnders G, Blank D H A and Ramesh R 2008 *Phys. Rev.* B **78** 094413

[14] Luo W, Pennycook S J and Pantelides S T 2008 *Phys. Rev. Lett.* **101** 247204

[15] Dagotto E, Hotta T and Moreo A 2001 *Phys. Rep.* **344** 1

[16] Dagotto E 2003 *Nanoscale Phase Separation and Colossal Magnetoresistance* (Heidelberg: Springer) p 1

[17] Zhang J, Bishop A R and Roder H 1996 *Phys. Rev.* B **53** 8840

[18] Holstein T 1959 *Ann. Phys.* **8** 325
Holstein T 1959 *Ann. Phys.* **8** 343

[19] Perroni C A, De Filippis G, Cataudella V and Iadonisi G 2001 *Phys. Rev.* B **64** 144302

[20] Lang I J and Firsov Yu A 1963 *Sov. Phys.—JETP* **16** 1301
Firsov Yu A 1975 *Polarons* (Moscow: Nauka)

[21] Das A N and Sil S 1993 *J. Phys.: Condens. Matter* **5** 8265

[22] Fang Z, Solovyev I V and Terakura K 2000 *Phys. Rev. Lett.* **84**

[23] Kubo K and Ohata N 1972 *J. Phys. Soc. Japan* **33** 21